

Magnetism in a lattice of spinor Bose condensates

Kevin Gross, Chris P. Search, Han Pu, Weiping Zhang and Pierre Meystre
Optical Sciences Center, The University of Arizona, Tucson, AZ 85721

(Dated: February 1, 2008)

We study the ground state magnetic properties of ferromagnetic spinor Bose-Einstein condensates confined in a deep optical lattices. In the Mott insulator regime, the “mini-condensates” at each lattice site behave as mesoscopic spin magnets that can interact with neighboring sites through both the static magnetic dipolar interaction and the light-induced dipolar interaction. We show that such an array of spin magnets can undergo a ferromagnetic or anti-ferromagnetic phase transition under the magnetic dipolar interaction depending on the dimension of the confining optical lattice. The ground-state spin configurations and related magnetic properties are investigated in detail.

PACS numbers: PACS numbers: 03.75.Fi, 75.45.+j, 75.60.Ej

I. INTRODUCTION

The interaction between quantum degenerate atomic gases and optical fields is a cornerstone of modern atomic physics and quantum optics. In early experiments on Bose-Einstein condensation, light fields were applied primarily for the capture and precooling of atoms, preceding the last stage of evaporative cooling in a magnetic trap. They were also used to obtain dramatic images of the condensates (BEC), and to launch solitons [1] and vortices [2] in condensates. This was soon followed by applications such as the trapping of condensates in optical dipole traps, and the demonstrations of matter-wave superradiance [3, 4] and of coherent matter-wave amplification [5]. More recently, optical dipole traps have been employed for the all-optical realization of BEC and of quantum-degenerate Fermi gases [6, 7].

Optical lattices, formed by counterpropagating laser beams in one, two and three dimensions, were originally used in polarization gradient cooling and sub-recoil cooling experiments at the single-atom level. They rapidly found further applications in the manipulation of BECs, first in the demonstration of a “mode-locked” atom laser and the observation of Josephson tunneling between lattice wells [8], and subsequently in the transport and acceleration of condensates [9]. More recently, they have lead to the demonstration of the superfluid-Mott insulator transition [10, 11], and of the collapse and revival of the condensate wave function [12]. In the near future, they may also prove useful in the realization of bright atomic solitons relying on negative effective atomic masses in periodic potentials [13].

In contrast to magnetic traps, which only capture atoms in weak-field seeking states, optical traps function for all hyperfine sublevels of the alkali electronic ground states. This presents considerable advantages, in particular in the study of spinor condensates such as sodium and rubidium. The first study of the magnetic properties of spinor condensates were carried out by Ketterle and coworkers, who investigated the existence of coexisting spin domains in ^{23}Na , an “anti-ferromagnetic”, or “polar” condensate [14].

Recent experimental and theoretical studies have es-

tablished that in contrast to ^{23}Na , ^{87}Rb is expected to be ferromagnetic at zero temperature. That is, the expectation value of its total spin \mathbf{F} is finite, $\langle \mathbf{F} \rangle \neq 0$ [15, 16, 17]. As a result, an ensemble of condensates placed at the potential minima of an optical lattice would act as mesoscopic magnets, much like large spins on a crystalline lattice. In the absence of external fields and long range site-to-site interactions, these magnets would have random orientations.

The situation is changed in the presence of interactions between neighboring lattice sites. It is known that in the case of spins on a crystal lattice, the dominant source of coupling is the quantum-mechanical exchange interaction. We recall that 19th century physics failed in its attempts to explain ferromagnetism in terms of the magnetic dipole-dipole interaction, and it is Heisenberg who first introduced the exchange force to explain this effect [18, 19]. In the present case, though, the overlap between neighboring condensate wave functions is negligible for deep enough lattice wells — the Mott insulator state — and so is the exchange interaction. Instead, the individual mesoscopic magnets are coupled by the magnetic (and possibly also the optical) dipole-dipole interaction. Because of the large number N of atoms at each lattice site, this interaction is no longer negligible, despite the large distance, of the order of half an optical wavelength, between sites. As such, the present situation is in some sense a return to 19th century physics. The goal of this paper is to discuss several aspects of the spin and magnetic properties of such lattice systems in one- and two-dimensions.

The remainder of the paper is organized as follows. Section II briefly reviews the theory of spinor condensates in general, with special emphasis on the ferromagnetic and polar ground states resulting from local spin-changing collisions. We then introduce the nonlocal long-range magnetic dipole-dipole interaction between condensates at different sites in the optical lattice. Section III briefly reviews previously published results on one-dimensional lattices, and discusses the ferromagnetic ground state of the full lattice. On this basis, an extension of the one-dimensional case to two-dimensional lattices are analyzed in section IV. The ground state of

the system is determined numerically using a genetic algorithm that is discussed in some detail. We show that in that case, the ground state is normally anti-ferromagnetic. Edge effects are also briefly addressed. Finally, Section V is a conclusion and outlook.

II. MODEL

The dynamics of spinor condensates trapped in optical lattices is primarily governed by three types of two-body interactions: spin-changing collisions, magnetic dipole-dipole interactions, and light-induced dipole-dipole interactions. For an optical lattice created by blue-detuned laser beams, the atoms are trapped in the dark-field nodes of the lattice and the light-induced dipole-dipole interaction can be neglected [20]. In this paper, we focus on this case. As a preparation for sections III, IV and V, we first discuss the interatomic interactions in some detail.

A. Spin-changing collisions

In second-quantized form, the Hamiltonian describing a system of spin $f = 1$ bosons subject to local spin-changing collisions is [21, 22, 23, 24]

$$\begin{aligned} \mathcal{H} = & \sum_{\alpha} \int d^3r \left(\frac{\hbar^2}{2M} \nabla \psi_{\alpha}^{\dagger}(\mathbf{r}) \cdot \nabla \psi_{\alpha}(\mathbf{r}) + U(\mathbf{r}) \psi_{\alpha}^{\dagger}(\mathbf{r}) \psi_{\alpha}(\mathbf{r}) \right) \\ & + \frac{c_0}{2} \sum_{\alpha, \beta} \int d^3r \psi_{\alpha}^{\dagger}(\mathbf{r}) \psi_{\beta}^{\dagger}(\mathbf{r}) \psi_{\beta}(\mathbf{r}) \psi_{\alpha}(\mathbf{r}) \\ & + \frac{c_2}{2} \sum_{\alpha, \beta, \mu, \nu} \int d^3r \psi_{\alpha}^{\dagger}(\mathbf{r}) \psi_{\beta}^{\dagger}(\mathbf{r}) \mathbf{F}_{\alpha, \mu} \cdot \mathbf{F}_{\beta, \nu} \psi_{\nu}(\mathbf{r}) \psi_{\mu}(\mathbf{r}), \end{aligned} \quad (1)$$

where $\psi_{\alpha}(\mathbf{r})$ is the field annihilation operator for an atom in the hyperfine state $|f = 1, m_f = \alpha\rangle$, $\alpha = -1, 0, 1$, $U(\mathbf{r})$ is a potential produced by an optical dipole trap and assumed to be the same for all hyperfine states, and M is the mass of the atoms. \mathbf{F} is the vector operator for the hyperfine spin of an atom, with components represented by 3×3 matrices in the $|f = 1, m_f = \alpha\rangle$ subspace. For ultracold bosons, only s -wave collisions with total hyperfine spin of $F = 0, 2$ are allowed, and

$$c_0 = \frac{4\pi\hbar^2}{3M} (a_0 + 2a_2),$$

and

$$c_2 = \frac{4\pi\hbar^2}{3M} (a_2 - a_0),$$

where a_0 and a_2 are the s -wave scattering lengths for collisions in the $F = 0$ and $F = 2$ channel, respectively.

The ground state properties of spinor condensates subject to these local spin-changing collisions have been determined by introducing the components $\phi_{\alpha}(\mathbf{r})$ of the

spinor condensate wave function in the mean-field approximation,

$$\phi_{\alpha}(\mathbf{r}) = \langle \psi_{\alpha}(\mathbf{r}) \rangle = \sqrt{n(\mathbf{r})} \zeta_{\alpha}(\mathbf{r}), \quad (2)$$

where $n(\mathbf{r})$ is the local atomic density and $\zeta_{\alpha}(\mathbf{r})$ a normalized spinor, and minimizing the energy functional

$$\begin{aligned} E = & \int d^3r \frac{\hbar^2}{2M} \left(\left(\nabla \sqrt{n(\mathbf{r})} \right)^2 + (\nabla \zeta(\mathbf{r}))^2 n(\mathbf{r}) \right) \\ & - \int d^3r \left[(\mu - U(\mathbf{r})) n(\mathbf{r}) - \frac{n^2(\mathbf{r})}{2} (c_0 + c_2 \langle \mathbf{F}(\mathbf{r}) \rangle^2) \right]. \end{aligned}$$

In this expression, μ is the chemical potential and the averaged single-atom spin angular momentum is

$$\langle \mathbf{F}(\mathbf{r}) \rangle = \sum_{\alpha, \beta} \zeta_{\alpha}^{\star}(\mathbf{r}) \mathbf{F}_{\alpha, \beta} \zeta_{\beta}(\mathbf{r}). \quad (3)$$

For $c_2 > 0$, the energy E is minimized by $\langle \mathbf{F}(\mathbf{r}) \rangle = 0$, and the spinor condensate is in an “anti-ferromagnetic”, or “polar” state. This is the case for ^{23}Na condensates, in which case $a_2 - a_0 \simeq 5$ a.u. Ketterle and coworkers have studied this situation in great detail [14]. In particular they have obtained spin-domain diagrams and studied experimentally the miscibility of these domains in the presence of external fields.

For $c_2 < 0$, in contrast, the energy E is minimized by making $\langle \mathbf{F}(\mathbf{r}) \rangle^2 = 1$. As discussed in Ref. [22], the direction of the spin is

$$\langle \mathbf{F}(\mathbf{r}) \rangle = \cos \beta_0 \hat{\mathbf{z}} + \sin \beta_0 \times (\cos \alpha_0 \hat{\mathbf{x}} + \sin \alpha_0 \hat{\mathbf{y}}), \quad (4)$$

where α_0 and β_0 are Euler angles. All possible orientations (α_0, β_0) are possible and lead to the same ground-state energy E . Recent theoretical calculations by Klausen *et al.* predict that for spin-1 ^{87}Rb , the scattering lengths a_0 and a_2 are almost equal, but with $a_0 > a_2$, with a difference of the order of 0.3 to 2.7 a.u. [16].

Consider, then, an ^{87}Rb condensate trapped on an optical lattice with wells deep enough that its ground state is the Mott-insulator state, i.e., there is no global phase of the condensate over many lattice sites [11]. Each lattice site is therefore the location of a “mini-condensate,” which can contain as many as several thousands atoms in one-dimensional lattices, and several hundreds in 2-D lattices. In the absence of external fields and long-range site-to-site interactions, these condensates can be thought of as independent magnets, whose spin vectors point in random directions, with no spin correlations between sites. This situation is similar to the spin lattices familiar from the study of magnetism, with two differences. First, the quantum mechanical exchange interaction, which is at the core of magnetism, is completely negligible in the present situation. This is because neighboring sites on an optical lattice are at least one half optical wavelength apart. For deep lattice wells, the center-of-mass wave functions for the individual mini-condensate

— essentially the ground state Wannier wave functions at the individual sites — do not have any significant overlap. Second, the magnetic dipolar coupling, which is normally negligible and leads to the prediction of Curie temperatures several orders of magnitude lower than actually observed in solid state magnetic materials, is now the dominant interaction, due to the large number N of atoms at each lattice site. This leads to an N^2 enhancement factor, as we now show.

B. Magnetic dipole-dipole interaction

In order to describe the magnetic dipolar interaction between mini-condensates at lattice sites \mathbf{i} and \mathbf{j} , we assume that the condensates at each site can be treated independently, and have the same spatial form, which is also independent of the spin state of the atoms. Specifically, we decompose the Schrödinger field operator as

$$\psi(\mathbf{r}) = \sum_{\alpha=0,\pm 1} \psi_{\alpha}(\mathbf{r})|f=1, m_f=\alpha\rangle,$$

with

$$\psi_{\alpha}(\mathbf{r}) = \sum_{\mathbf{i}} \phi_{\mathbf{i}}(\mathbf{r}) \hat{a}_{\alpha}(\mathbf{i}). \quad (5)$$

In this expansion, which goes beyond the mean-field approximation of Eq. (2), $\mathbf{r}_{\mathbf{i}}$ is the coordinate of the \mathbf{i} -th lattice site, $\hat{a}_{\alpha}(\mathbf{i})$ and $\hat{a}_{\alpha}^{\dagger}(\mathbf{i})$ are bosonic annihilation and creation operators for atoms in the hyperfine state α at site \mathbf{i} , and $\phi_{\mathbf{i}}(\mathbf{r}) = \phi(\mathbf{r} - \mathbf{r}_{\mathbf{i}})$ is the ground state wave function of the mini-condensate at that site, normalized to unity. For $a_0 \simeq a_2$, it is approximately given by the solution of the stationary Gross-Pitaevskii equation

$$\left[-\frac{\hbar^2 \nabla^2}{2M} + U_{\mathbf{i}}(\mathbf{r}) + c_0(N_{\mathbf{i}} - 1)|\phi_{\mathbf{i}}(\mathbf{r})|^2 - \mu \right] \phi_{\mathbf{i}}(\mathbf{r}) = 0,$$

where

$$N_{\mathbf{i}} = \sum_{\alpha} \langle \hat{a}_{\alpha}^{\dagger}(\mathbf{i}) \hat{a}_{\alpha}(\mathbf{i}) \rangle,$$

is the total number of atoms at site \mathbf{i} and we assume that all sites have the same number of atoms.

The magnetic dipole-dipole interaction between the mini-condensates at sites \mathbf{i} and \mathbf{j} is given by [25]

$$V_{dd}^{\mathbf{ij}} = \frac{\mu_0}{4\pi} \int d^3r \int d^3r' |\phi(\mathbf{r} - \mathbf{r}_{\mathbf{i}})|^2 |\phi(\mathbf{r}' - \mathbf{r}_{\mathbf{j}})|^2 \times \left[\frac{\vec{\mu}_{\mathbf{i}} \cdot \vec{\mu}_{\mathbf{j}}}{|\mathbf{r} - \mathbf{r}'|^3} - \frac{3(\vec{\mu}_{\mathbf{i}} \cdot (\mathbf{r} - \mathbf{r}'))(\vec{\mu}_{\mathbf{j}} \cdot (\mathbf{r} - \mathbf{r}'))}{|\mathbf{r} - \mathbf{r}'|^5} \right],$$

where μ_0 is the vacuum permeability and $\vec{\mu}_{\mathbf{i}}$ is the magnetic dipole moment at site \mathbf{i} . In second-quantized form, it is given explicitly by

$$\vec{\mu}_{\mathbf{i}} = \gamma_B \sum_{\alpha,\beta} \hat{a}_{\alpha}^{\dagger}(\mathbf{i}) \mathbf{F}_{\alpha,\beta} \hat{a}_{\beta}(\mathbf{i}) \equiv \gamma_B \mathbf{S}_{\mathbf{i}},$$

where $\gamma_B = g_F \mu_B$ is the gyromagnetic ratio and we recognize that $\mathbf{S}_{\mathbf{i}}$ is the angular momentum operator for the condensate at site \mathbf{i} . We remark that for a given site, the expectation value of $\vec{\mu}_{\mathbf{i}}$ is

$$\begin{aligned} \langle \vec{\mu}_{\mathbf{i}} \rangle &= \gamma_B \sum_{\alpha,\beta} \langle \hat{a}_{\alpha}^{\dagger}(\mathbf{i}) \mathbf{F}_{\alpha,\beta} \hat{a}_{\beta}(\mathbf{i}) \rangle \\ &\simeq N_{\mathbf{i}} \gamma_B \langle \mathbf{F}_{\mathbf{i}} \rangle, \end{aligned}$$

where $\langle \mathbf{F}_{\mathbf{i}} \rangle$ is the single-atom magnetization at the site, see Eq. (3).

Summarizing, then, the Hamiltonian describing the spinor “mini-condensates” in the optical lattice, subject to spin-changing collisions and to an inter-site magnetic dipolar interaction has the spin-spin coupling form

$$H = \sum_{\mathbf{i}} \left[\lambda'_{\mathbf{i}} \mathbf{S}_{\mathbf{i}}^2 + \gamma_B \sum_{\mathbf{j} \neq \mathbf{i}} \lambda_{\mathbf{ij}} \mathbf{S}_{\mathbf{i}} \cdot \mathbf{S}_{\mathbf{j}} - 3\gamma_B \sum_{\mathbf{j} \neq \mathbf{i}} \mathbf{S}_{\mathbf{i}} \cdot \Lambda_{\mathbf{ij}} \cdot \mathbf{S}_{\mathbf{j}} - \gamma_B \mathbf{S}_{\mathbf{i}} \cdot \mathbf{B}_{\text{ext}} \right], \quad (6)$$

where

$$\begin{aligned} \lambda'_{\mathbf{i}} &= (1/2)c_2 \int d^3r |\phi(\mathbf{r} - \mathbf{r}_{\mathbf{i}})|^4, \\ \lambda_{\mathbf{ij}} &= \frac{\gamma_B \mu_0}{4\pi} \int d^3r \int d^3r' \frac{|\phi(\mathbf{r} - \mathbf{r}_{\mathbf{i}})|^2 |\phi(\mathbf{r}' - \mathbf{r}_{\mathbf{j}})|^2}{|\mathbf{r} - \mathbf{r}'|^3} \end{aligned}$$

and the tensor $\Lambda_{\mathbf{ij}}$ is defined by

$$\Lambda_{\mathbf{ij}} = \frac{\gamma_B \mu_0}{4\pi} \int d^3r \int d^3r' \frac{|\phi(\mathbf{r} - \mathbf{r}_{\mathbf{i}})|^2 |\phi(\mathbf{r}' - \mathbf{r}_{\mathbf{j}})|^2 (\mathbf{r} - \mathbf{r}')^2}{|\mathbf{r} - \mathbf{r}'|^5}.$$

We have also introduced an external magnetic field \mathbf{B}_{ext} for future use. In the limit of tight confinement, the condensate wave functions at each lattice site can be approximated by

$$|\phi(\mathbf{r} - \mathbf{r}_{\mathbf{i}})|^2 \approx \delta(\mathbf{r} - \mathbf{r}_{\mathbf{i}}).$$

In this limit we have

$$\lambda_{\mathbf{ij}} = \frac{\gamma_B \mu_0}{4\pi |\mathbf{r}_{\mathbf{ij}}|^3},$$

and the tensor $\Lambda_{\mathbf{ij}}$ becomes

$$\Lambda_{\mathbf{ij}} = \lambda_{\mathbf{ij}} \hat{\mathbf{r}}_{\mathbf{ij}}^2,$$

where $\mathbf{r}_{\mathbf{ij}} = \mathbf{r}_{\mathbf{i}} - \mathbf{r}_{\mathbf{j}}$ and $\hat{\mathbf{r}}_{\mathbf{ij}} = \mathbf{r}_{\mathbf{ij}}/|\mathbf{r}_{\mathbf{ij}}|$.

III. FERROMAGNETISM IN A 1D OPTICAL LATTICE

In this section, we study the magnetic properties and spin dynamics of spinor condensates in a 1D optical lattice. More specifically, we consider a blue-detuned optical lattice where the mini-condensates are trapped at the

standing wave nodes. In this case, the light-induced dipolar interaction can be ignored and the mini-condensates only interact via the magnetic dipolar interaction. Without loss of generality, we assume that the axis of the lattice is along the z direction, which we also choose as the quantization axis. Hence the total Hamiltonian (6) reduces to

$$H = \sum_i \left[\lambda'_a \mathbf{S}_i^2 + \gamma_B \sum_{j \neq i} \lambda_{ij} \mathbf{S}_i \cdot \mathbf{S}_j - 3\gamma_B \sum_{j \neq i} \lambda_{ij} S_i^z S_j^z - \gamma_B \mathbf{S}_i \cdot \mathbf{B}_{\text{ext}} \right]. \quad (7)$$

We assume that the magnetic field \mathbf{B}_{ext} is of the form

$$\mathbf{B}_{\text{ext}} = B_z \hat{\mathbf{z}} + B_x \hat{\mathbf{x}},$$

where $B_z \hat{\mathbf{z}}$ is an applied field and $B_x \hat{\mathbf{x}}$ is an effective magnetic field that accounts for all possible effects from the experimental environment. While this field can have any possible orientation, we take it to be transverse and along $\hat{\mathbf{x}}$ without loss of generality, since any longitudinal component can be included in B_z .

Furthermore, we consider an infinitely long lattice so that boundary effects can be ignored. The hamiltonian describing the spin \mathbf{S} of a generic site i reads then

$$h = \lambda'_a \mathbf{S}^2 - \gamma_B \mathbf{S} \cdot \left[\left(B_z + 2 \sum_{j \neq i} \lambda_{ij} S_j^z \right) \hat{\mathbf{z}} + \left(B_x - \sum_{j \neq i} \lambda_{ij} S_j^x \right) \hat{\mathbf{x}} - \sum_{j \neq i} \lambda_{ij} S_j^y \hat{\mathbf{y}} \right]. \quad (8)$$

We now proceed to determine the ground state of the single-site Hamiltonian (8) in the mean-field — or Weiss molecular field — approximation [19]. It consists in replacing the operators S_j^α , $\alpha = x, y, z$, by their ground-state expectation value

$$\langle S_j^\alpha \rangle \rightarrow M_\alpha = N m_\alpha, \quad (9)$$

which is assumed to be the same for all sites. We remark that m_z is nothing but the difference in population of the Zeeman sublevels of magnetic quantum numbers ± 1 . Replacing S_j^α by $N m_\alpha$ allows us to approximate the Hamiltonian (8) by

$$h_{\text{mf}} = \lambda'_a \mathbf{S}^2 - \gamma_B \mathbf{S} \cdot \mathbf{B}_{\text{eff}}, \quad (10)$$

where we have introduced the effective magnetic field

$$\mathbf{B}_{\text{eff}} = (B_z + 2\Lambda m_z) \hat{\mathbf{z}} + (B_x - \Lambda m_x) \hat{\mathbf{x}} - \Lambda m_y \hat{\mathbf{y}},$$

and

$$\Lambda = N \sum_{j \neq i} \lambda_{ij}.$$

In the case of ^{87}Rb , the individual spinor condensates at the lattice sites are ferromagnetic, $\lambda'_a < 0$. In that case, the ground state of the mean-field Hamiltonian (10) must correspond to a situation where the condensate at the site i under consideration must be aligned along \mathbf{B}_{eff} and takes its maximum possible value N . That is, the ground state of the mean-field Hamiltonian (10) is simply

$$|GS\rangle = |N, N\rangle_{\mathbf{B}_{\text{eff}}}, \quad (11)$$

where the first number denotes the total angular momentum and the second its component along the direction of \mathbf{B}_{eff} . Note that $|GS\rangle$ represents a spin coherent state in the basis of $|S, S_z\rangle$. The fact that the ground state magnetic dipole moment of each lattice site is N times that of an individual atom results in a significant magnetic dipole-dipole interaction even for lattice points separated by hundreds of nanometers. This feature, which can be interpreted as a signature of Bose enhancement, is in stark contrast with usual ferromagnetism, where the magnetic interaction is negligible compared to exchange and where the use of fermions is essential.

The mean-field ground state of Eq. (11) allows us to calculate the magnetization $m_{x,y,z}$. One finds readily

$$m_\alpha = \frac{1}{N} \langle GS | S_i^\alpha | GS \rangle = \cos \theta_\alpha,$$

where θ_α is the angle between \mathbf{B}_{eff} and the α -axis. In the absence of externally applied field, $B_z = 0$, this gives

$$m_z = \frac{2\Lambda m_z}{B}, \quad (12a)$$

$$m_x = \frac{B_x - \Lambda m_x}{B}, \quad (12b)$$

$$m_y = -\frac{\Lambda m_y}{B} \quad (12c)$$

where $B = \sqrt{(2\Lambda m_z)^2 + (B_x - \Lambda m_x)^2 + (\Lambda m_y)^2}$ normalizes the magnetization vector to unity.

Since $B > 0$, the third of these equations implies that $m_y = 0$. With $m_x^2 + m_z^2 = 1$ and the condition $2\Lambda = B$, which follows directly from the equation for m_z , we find further that for $B_x \geq 3\Lambda$, the unique solution is $m_z = m_y = 0$, $m_x = 1$. That is, the lattice of condensates is magnetically polarized along the environmental magnetic field B_x . For $B_x < 3\Lambda$, in contrast, there are two coexisting sets of solutions: i) $m_z = m_y = 0$ and $m_x = 1$; and ii) $m_z = \pm \sqrt{1 - (B_x/3\Lambda)^2}$, $m_y = 0$ and $m_x = B_x/3\Lambda$. It is easily seen that the state associated with the latter solutions has the lower energy. Hence it corresponds to the true ground state, while solution 1 represents an unstable equilibrium.

We have, then, the following situation: As the effective magnetic field strength B_x is reduced below the critical value 3Λ , the lattice ceases to be polarized along the direction of that field. A phase transition occurs, and a *spontaneous magnetization* along the z -direction appears, characterized by a finite m_z . This phenomenon

is reminiscent of conventional ferromagnetism. Indeed, our model is analogous to the Ising model[18], with the environmental transverse magnetic field B_x playing the role of temperature. For $B_x = 0$ — corresponding to zero temperature in Ising model — the spins at each lattice site \mathbf{S}_i align themselves along the lattice direction, even in the absence of longitudinal field. This spontaneous spin magnetization diminishes as B_x increases, and completely vanishes if B_x exceeds the critical value 3Λ — the analog of the Curie temperature in the Ising model. We note however that the situation at hand exhibits important qualitative differences with the Ising model. For example, no spontaneous magnetization occurs in 1D Ising model, for any finite temperature.

We note however that the appearance of a spontaneous magnetization does not rely on this condition being fulfilled. This point was discussed in Ref.[27], which numerically solved the Hamiltonian (7) without invoking the mean-field approximation for a two-well system and showed how the situation rapidly approaches the mean-field results as N increases.

IV. ANTI-FERROMAGNETIC GROUND STATE OF THE 2D LATTICE

Now we turn our attention to 2D lattices, formed as before by blue-detuned lasers. We show that depending on the relative magnitude of the lattice constants along its two axes, this system exhibits a variety of possible ground states, including an anti-ferromagnetic configuration.

We consider a rectangular lattice in the (y, z) -plane, with primitive lattice vectors $\mathbf{a} = a\hat{\mathbf{z}}$ and $\mathbf{b} = b\hat{\mathbf{y}}$, of lengths a and b , in these two directions. We assume as before that the number of atoms at each lattice site is the same and that the atoms are tightly confined so that we can approximate their probability density by a delta function at each lattice site,

$$|\phi_{ij}(\mathbf{r})|^2 = \delta(\mathbf{r} - \mathbf{r}_{ij}).$$

Here, $\mathbf{r}_{ij} = i\mathbf{a} + j\mathbf{b}$ is the position of the center of the (i, j) lattice site. Under these conditions, the Hamiltonian (6) with $\mathbf{B}_{\text{ext}} = 0$ becomes

$$H = \sum_{ij} \left[\frac{\lambda_a}{2} \mathbf{S}_{ij}^2 + \frac{\gamma B \mu_0}{4\pi} \sum_{kl \neq ij} \mathbf{S}_{ij}^T \cdot \Lambda_{ij,kl} \cdot \mathbf{S}_{kl} \right] \quad (13)$$

where

$$\Lambda_{ij,kl} = \begin{pmatrix} \frac{1}{|\mathbf{r}_{ij,kl}|^3} & 0 & 0 \\ 0 & \frac{1}{|\mathbf{r}_{ij,kl}|^3} - \frac{3(na)^2}{|\mathbf{r}_{ij,kl}|^5} & -\frac{3(na)(mb)}{|\mathbf{r}_{ij,kl}|^5} \\ 0 & -\frac{3(na)(mb)}{|\mathbf{r}_{ij,kl}|^5} & \frac{1}{|\mathbf{r}_{ij,kl}|^3} - \frac{3(mb)^2}{|\mathbf{r}_{ij,kl}|^5} \end{pmatrix}. \quad (14)$$

and $\mathbf{r}_{ij,kl} = \mathbf{r}_{ij} - \mathbf{r}_{kl} = n\mathbf{a} + m\mathbf{b}$, with $n = i - k$ and $m = j - l$.

A. infinite size lattices

As in the preceding section, we determine the ground state of the lattice in the semiclassical limit, ignoring spin-spin correlations and replacing the operators \mathbf{S}_{ij} with their expectation value with respect to a spin coherent state,

$$\mathbf{S}_{ij} \rightarrow \langle \mathbf{S}_{ij} \rangle = \mathbf{M}_{ij}.$$

The semiclassical ground state corresponds to the orientation of the spin vectors that minimizes the semiclassical energy corresponding to the Hamiltonian (13). In contrast to the one-dimensional case, it is not obvious from inspection of Eq. (13) that all expectation values \mathbf{M}_{ij} should be equal. Hence, the determination of the ground state for an $N \times M$ lattice requires the minimalization of the energy with respect to $2NM$ variables. However, in the limit of an infinite lattice the ground state should be translationally invariant with respect to displacements of the spins by a finite number of lattice constants along either axis. We can therefore generalize the mean-field ansatz used in the one-dimensional case by assuming that the 2D lattice can be decomposed into a finite set $\{\ell\}$ of interpenetrating periodic sublattices for which all spin vectors have the same orientation.

The positions of the sites of the sublattice ℓ of primitive lattice vectors \mathbf{a}_ℓ and \mathbf{b}_ℓ are

$$\mathbf{r}_{\ell,ij} = i\mathbf{a}_\ell + \mathbf{a}_{\ell,0} + j\mathbf{b}_\ell + \mathbf{b}_{\ell,0}$$

where $\mathbf{a}_{\ell,0}$ and $\mathbf{b}_{\ell,0}$ denote the origin of that lattice. Since the interaction between dipole moments that are perpendicular to the plane of the lattice is repulsive while the interaction between dipole moments in the plane of the lattice is predominantly attractive, the ground state must correspond to spin vectors in the plane (y, z) of the lattice. Hence the spin vector associated with the sublattice ℓ can be written as

$$\mathbf{M}_\ell = N (\cos \theta_\ell \hat{\mathbf{y}} + \sin \theta_\ell \hat{\mathbf{z}}).$$

One can gain an intuitive feel for the ground state of the system by considering what happens when one lets a 1D lattice approach an already existing one from infinity. For concreteness, we take the axes of both lattices to be along $\hat{\mathbf{z}}$. We know from the previous section that for large lattice separations, the spins in each lattice will be oriented in either the $+\hat{\mathbf{z}}$ or $-\hat{\mathbf{z}}$ direction with equal probability. In effect, each lattice acts like a long bar magnet. As the lattices approach each other, though, they start to interact via their magnetic dipole moments. The minimization of energy then proceeds in a familiar way: Just as two bar magnets placed side by side orient themselves so that opposite poles are next to each other, the spins of the two 1D lattices will arrange their orientation so that the spins in one lattice point along $+\hat{\mathbf{z}}$ while in the other lattice the spins point along $-\hat{\mathbf{z}}$. This will remain true as long as the lattice separation is much larger than

the primitive lattice vector \mathbf{b} of the 1D lattices, due to the $1/r^3$ dependence of the magnetic dipole interaction. Indeed, in this case the easy axis is the y -axis.

This argument can easily be generalized to many rows. It follows that for $a \gg b$, rows of spins parallel to the z -axis will alternatively align themselves along the $+\hat{\mathbf{z}}$ and $-\hat{\mathbf{z}}$ direction. Similarly, for $a \ll b$, the z -axis becomes the easy axis and rows of spins parallel to y align themselves alternatively along the $+\hat{\mathbf{y}}$ or $-\hat{\mathbf{y}}$ direction. In both cases, though, the ground state is expected to be anti-ferromagnetic.

Even though the magnetic dipole interaction is long ranged, it is easy to see that neighboring spins within each row interact more strongly than do neighboring spins in adjacent rows provided that $a = b + \epsilon$ with ϵ positive. One therefore expects that the ground state will remain anti-ferromagnetic unless $\epsilon \rightarrow 0$. In this limit, there are clearly two degenerate anti-ferromagnetic ground states that are topologically distinct, i.e. that can not be related by a simple rotation. Any weighted combination of these two configurations has the same energy and is therefore a new degenerate ground state. Assigning the weight $\cos^2 \theta$ to the ground state with all spins pointing in the $\pm \hat{\mathbf{y}}$ direction and $\sin^2 \theta$ to the ground state with all spins in the $\pm \hat{\mathbf{z}}$, then we find that this situation is equivalent to a ground state consisting of four interpenetrating sublattices ($\ell = 1, 2, 3, 4$), with spin orientations,

$$M_1 = N(\cos \theta \hat{\mathbf{y}} + \sin \theta \hat{\mathbf{z}}), \quad (15a)$$

$$M_2 = N(-\cos \theta \hat{\mathbf{y}} + \sin \theta \hat{\mathbf{z}}), \quad (15b)$$

$$M_3 = N(-\cos \theta \hat{\mathbf{y}} - \sin \theta \hat{\mathbf{z}}), \quad (15c)$$

$$M_4 = N(\cos \theta \hat{\mathbf{y}} - \sin \theta \hat{\mathbf{z}}), \quad (15d)$$

and sublattice sites located at

$$\mathbf{r}_{1,ij} = 2i\mathbf{a} + 2j\mathbf{b}, \quad (16a)$$

$$\mathbf{r}_{2,ij} = 2i\mathbf{a} + (2j+1)\mathbf{b}, \quad (16b)$$

$$\mathbf{r}_{3,ij} = (2i+1)\mathbf{a} + (2j+1)\mathbf{b}, \quad (16c)$$

$$\mathbf{r}_{4,ij} = (2i+1)\mathbf{a} + 2j\mathbf{b}, \quad (16d)$$

where $i, j = 0, \pm 1, \pm 2, \dots$. The corresponding lattice structure is illustrated in Fig. 1. For $a = b$ all values of θ are degenerate while for $a < b$ and $a > b$ the ground state corresponds to θ equal to 0 and $\theta = \pi/2$, respectively.

The next section discusses the use of a genetic algorithm to numerically determine of the lattice ground state for a finite lattice size.

B. Finite size lattices

1. Genetic algorithm

Genetic algorithms have become a widely used tool for solving optimization problems that depend on a large

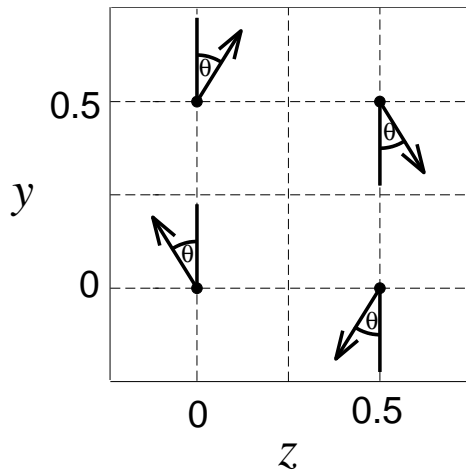


FIG. 1: Orientations of the spins on the four interpenetrating sublattices for $a = b$. The lengths are in units of λ .

number of variables [28]. The basic idea behind genetic algorithms is Darwinian natural selection. These algorithms proceed from an initial set of trial solutions to the optimization problem, which can be thought of as individuals in a population. The individuals breed, following some prescribed mating rules, to produce offspring, which constitute the next generation of individuals. In addition, random mutations are also introduced. The offspring that produce better solutions to the problem survive and are allowed to further breed, while those that produce poor solutions are eliminated. Ideally, after many generations the algorithm converges to the optimal solution(s) to the problem at hand.

In the specific system at hand, the algorithm starts from a large population \mathcal{N} of initial lattices, typically $\mathcal{N} = 512$. Most of them have completely random spin orientations, but some may have ordered configurations based on the ground state of the infinite lattice. At each generation, the genetic algorithm performs a combination of mutations and breeding steps on the members of the population, which we refer to as mutating and mating.

The mutations modify each member of the population to form a second population of \mathcal{N} lattices. They can be either global and local. Local mutations involve giving random rotations to a random percentage of the spins in the individual lattices. These rotations are by angles φ and θ about the y and x axes, respectively, where φ and θ are normally distributed random numbers with standard deviations typically chosen to be $\pi/8$. In contrast, the global mutations rotate *all* spin in the lattice by related amounts: They either apply the same random rotation to all lattice sites, or rotate the spin at each lattice site by a slightly different amount determined by its value (this is used when investigating the case of equal lattice constants, $a = b$, discussed below). In general, a given individual is subjected to both local and global mutations.

After the mutations are performed, the $2\mathcal{N}$ individuals are allowed to mate. The mating process randomly

picks two individuals using a normally distributed probability distribution centered around individuals with the lowest energy. This insures that, on average, only those individuals with the lowest energies produce offspring. Each pair of parents produces two offsprings using one of four randomly selected mating techniques: site swapping, sub-lattice swapping, row and column swapping, and row and column rearranging. Site swapping consists of swapping a random number of randomly chosen sites from the parents. Similarly, sub-lattice swapping consists of swapping a randomly sized and positioned sub-lattice between the parents. Row and column swapping works by randomly picking rows from both parents and forming one child, and doing the same with columns to form a second child. Row and column rearranging uses only a single parent to produce a child by randomly rearranging its rows or columns. The mating process is repeated \mathcal{N} times at each generation to produce a total population of $4\mathcal{N}$ lattices. Of those, only the \mathcal{N} individuals with the lowest energy are selected as parents for the next generation.

The genetic algorithm is run until the relative energies of the individuals in generation \mathcal{M} and $\mathcal{M} - 100$ differ by less than 10^{-7} .

2. Numerical results

The ground state of the system determined by the genetic algorithm is characterized by all spins lying in the plane of the lattice, in agreement with the discussion of section IV. If the lengths of the primitive lattice vectors a and b differ significantly, say, by 10 percent or more, the ground state is anti-ferromagnetic. With the exception of sites near the lattice boundary, the anti-ferromagnetic structure is identical to that predicted based on an infinite lattice.

As is to be expected, boundary effects become more important, the smaller the lattice. In that case, the ground state is characterized by spins orientations near the boundaries that deviate from the $\pm\hat{y}$ or $\pm\hat{z}$ directions. When a and b are significantly different, these boundary effects are manifest only near the corners of the lattice, and they lower the ground state energy by a very small amount. For example, for $a = 0.6\lambda$ and $b = 0.5\lambda$, where λ is the wavelength of the laser forming the lattice in the z -direction, the boundary effects reduce the ground-state energy of an 11×11 lattice by only 0.1 percent compared to its infinite lattice value. For larger lattices, the boundary effects become even smaller.

When $a = b$, finite size effects are more important in determining the spin structure of the ground state. We recall that in that case, an infinite lattice possesses an infinite number of degenerate ground states characterized by the angle θ . Boundary effects break this degeneracy and lead to the appearance of a preferred pattern. Fig. 2 illustrates the transition from the boundary dominated pattern of the $a = b$ situation to the anti-ferromagnetic

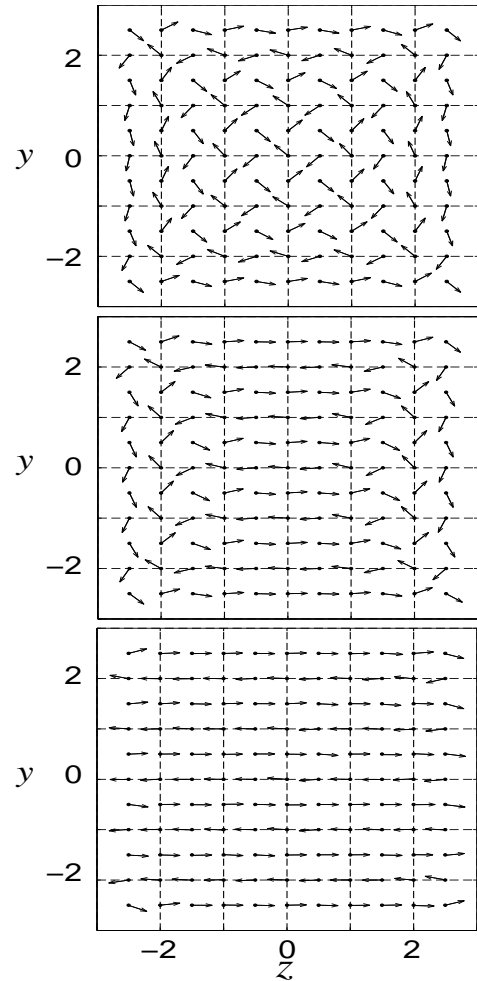


FIG. 2: The ground state configuration shows the transition from the boundary dominated pattern for $a = b$ to the anti-ferromagnetic configuration for $a \neq b$. From top to bottom, $b = 0.5, 0.505$ and 0.6 , respectively and $a = 0.5$ for all figures. The lengths are in units of λ .

configuration of $a \neq b$. As illustrated in Fig. 2a, for the case of $a = b$, near boundaries the spins are aligned parallel to them. That this should be the case is plausible since when going from a situation where $a < b$ to $a > b$, the spin orientation must go from being parallel to the y -axis to being parallel to the z -axis. To accommodate the orthogonal directions along two adjacent boundaries, the angle θ near the corners changes in such a way that the spins at the corner sites make an angle of $\pi/4$ relative to the y - and z -axis. This lifts the degeneracy present in the infinite lattice. As a result, the spins near the center of the finite lattice always take on an orientation corresponding to Eqs. (15) and (16) with $\theta = \pi/4$. This result holds for all finite-size lattices. Finally, we note that the ground-states of finite-size lattices are two-fold degenerate, the second ground state being obtained by reflections about the y and z axes.

Figure 3 shows how the spins orient themselves as b

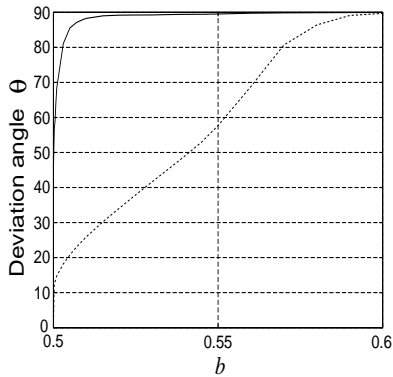


FIG. 3: Plot of the deviation angle θ relative to the y axis for the spin at the center of the lattice (solid curve) and a spin on left boundary of the lattice (dashed curve) as functions of b for fixed $a = 0.5$. Lengths are in units of λ .

changes for fixed a . As b deviates from a , the spins near the center of the lattice quickly become parallel to the easy-axis, while the spins near the boundaries become so much more slowly.

V. SUMMARY AND OUTLOOK

In summary, we have studied the spin configurations and magnetic properties of spinor Bose-Einstein condensates in an optical lattice. In the tight-binding limit, the ground state is the Mott-insulator state and the condensed atoms at each lattice site collectively behave as a spin magnet. Due to Bose enhancement, the dipole-dipole interactions between these spin magnets become important and may give rise to a rich variety of phenomena. We have shown here that the array of spin magnets can undergo a ferromagnetic (in the 1D case) or anti-ferromagnetic (in the 2D case) phase transition under the dipolar interaction when external magnetic fields are sufficiently weak. Using the same mechanism, it will also be possible to create ferrimagnetic lattice systems if one can interleave two sets of optical dipole potentials, each trapping one species of atoms (or one hyperfine state of the same atom) different from the other.

In the case of a far red-detuned lattice such that the spacing between adjacent lattice site exceeds the atomic resonant wavelength, the detection of the ground state spin structure amounts to detecting populations in the individual Zeeman sublevels at each site. This can be achieved using a Raman scattering scheme. For example, one can shine two light beams, one π -polarized and the other circularly polarized, onto the system. The absorption or gain of the probing light after passing the sample

is then a measure of the relative population of the hyperfine levels, since it depends upon which of them are initially populated. This scheme wouldn't work for a blue detuned lattice, though, since in that case the spacing between neighboring sites is sub-wavelength. However, the long range periodic spin structure, in particular the ferromagnetic and anti-ferromagnetic ordering, can still be detected by Bragg scattering [29]. Let us take ^{87}Rb as an example. Its ground state is the $5S_{1/2}$ state with $F = 1$. For σ^+ -polarized Bragg probe light (we choose the quantization axis to be parallel or antiparallel to atomic spins) with a frequency close to the $F = 1 \rightarrow F' = 2$ D2 resonance line, then the ratio of the transition strength (or scattering cross section) for atoms in $m = -1$ and $m = 1$ Zeeman sublevel is $1/6$. As a result, the Bragg signal depends on whether one has a ferromagnetic lattice (where all the atoms are in either $m = -1$ or $m = 1$ Zeeman sublevel) or anti-ferromagnetic lattice (where half the atoms are in $m = -1$ and the other half are in $m = 1$ sublevel).

In addition to their ground state structure, spinor condensates in an optical lattices also possesses considerable potential for studying other phenomena such as spin waves [30], macroscopic magnetization tunneling [31], domain wall formation, etc. Future studies will also include the dynamical properties of the system. Due to the long-range as well as the nonlinear nature of the dipolar interaction, the dynamics of the system should be very rich. For instance, given a ground state 2D lattice with primitive lattice constants $a < b$ where all the spins are aligned along the $\pm\hat{y}$ direction, one can suddenly modify the lattice light so that $a > b$. Whether and how the spins adjust themselves to the new ground state will be an interesting problem, closely related to the phenomenon of spin tunneling [31]. In addition, these systems may also find applications in the field of quantum information and computation. We conclude by noting that in addition to the Mott insulator limit studied in this paper, the genetic algorithm that we have developed here might be modified to investigate the other limit where tunneling between lattice sites becomes significant and the system becomes a superfluid [32].

Acknowledgments

We thank Prof. Poul Jessen for helpful discussion and S. Pötting for help with the figures. This work is supported in part by the US Office of Naval Research under Contract No. 14-91-J1205, by the National Science Foundation under Grants No. PHY00-98129, by the US Army Research Office, by NASA Grant No. NAG8-1775, and by the Joint Services Optics Program.

[1] S. Burger *et al.*, Phys. Rev. Lett. **82** 5198 (1999); J. Denschlag *et al.*, Science **287**, 97 (2000).

[2] M. R. Matthews *et al.*, Phys. Rev. Lett. **83**, 2498 (1999).

- [3] S. Inouye *et al.*, Science **285**, 571 (1999);
- [4] M. G. Moore and P. Meystre, Phys. Rev. Lett. **83**, 5202 (1999).
- [5] S. Inouye *et al.*, Nature (London) **402**, 641 (1999); M. Kozuma *et al.*, Science **286**, 2309 (1999).
- [6] M. D. Barrett, J. A. Sauer and M. S. Chapman, Phys. Rev. Lett. **87**, 010404 (2001).
- [7] S. R. Granade, M. E. Gehm, K. M. O'Hara and J. E. Thomas, Phys. Rev. Lett. **88**, 120405 (2002).
- [8] B. P. Anderson and M. A. Kasevich, Science **281**, 1686 (1998).
- [9] O. Morsch *et al.* Phys. Rev. Lett. **87**, 140402 (2001); S. Potting *et al.*, Phys. Rev. A **64**, 023604 (2001).
- [10] M. Greiner *et al.*, Nature (London) **415**, 39 (2002).
- [11] D. Jaksch *et al.*, Phys. Rev. Lett. **81**, 3108 (1998).
- [12] M. Greiner, O. Mandel, T. Hänsch and I. Bloch, private communication.
- [13] O. Zobay, S. Pötting, P. Meystre and E. M. Wright, Phys. Rev. A, 643 (1999); S. Pötting, O. Zobay, P. Meystre and E. M. Wright, J. Mod. Optics **47**, 2653 (2000).
- [14] J. Stenger *et al.*, Nature (London) **396**, 345 (1998).
- [15] J. P. Burke, Jr. and J. L. Bohn, Phys. Rev. A **59**, 1303 (1999).
- [16] N. N. Klausen, J. L. Bohn and C. H. Greene, Phys. Rev. A **64**, 053602 (2001).
- [17] E. G. M. van Kempen, S. J. J. M. F. Kokkelmans, D. J. Heinzen and B. J. Verhaar, Phys. Rev. Lett. **88**, 093201 (2002).
- [18] Kerson Huang, *Statistical Mechanics* (John Wiley & Sons, New York, 1987).
- [19] N. W. Ashcroft and N. D. Mermin, *Solid State Physics* (Harcourt Brace College Publishers, New York, 1976).
- [20] For a red-detuned lattice, the atoms are trapped in the antinodes of lattice laser beams and for appropriate laser parameters, the light-induced dipole-dipole interaction can have an important effect on spin dynamics as studied in Ref.[30].
- [21] W. Zhang and D. F. Walls, Phys. Rev. A **57**, 1248 (1998).
- [22] T. -L. Ho, Phys. Rev. Lett. **81**, 742 (1998).
- [23] T. Ohmi and K. Machida, J. Phys. Soc. Jpn. **67**, 1882 (1998).
- [24] C. K. Law, H. Pu and N. P. Bigelow, Phys. Rev. Lett. **81**, 5257 (1998).
- [25] The effect of the dipolar interaction on a condensate trapped in a single well has been considered by several groups. See, for example, K. Goral *et al.*, Phys. Rev. A **61**, 051601 (2000); L. Santos *et al.*, Phys. Rev. Lett. **85**, 1791 (2000); S. Yi and L. You, Phys. Rev. A **63**, 053607 (2001).
- [26] D. R. Meacher *et al.*, Phys. Rev. Lett. **74**, 1958 (1995).
- [27] H. Pu, W. Zhang and P. Meystre, Phys. Rev. Lett. **87**, 140405 (2001).
- [28] David Coley, *An Introduction to Genetic Algorithms for Scientists and Engineers* (World Scientific, Singapore, 1999).
- [29] G. Birkel *et al.*, Phys. Rev. Lett. **75**, 2823 (1995); M. Weidemüller *et al.*, Phys. Rev. Lett. **75**, 4583 (1995).
- [30] W. Zhang, H. Pu, C. Search and P. Meystre, Phys. Rev. Lett. **88**, 060401 (2002).
- [31] H. Pu, W. Zhang and P. Meystre, e-print cond-mat/0203066.
- [32] K. Goral, L. Santos and M. Lewenstein, Phys. Rev. Lett. **88**, 170406 (2002).